Motorised Shoe Mechanisms to Apply Chaotic Perturbations for Gait Training

David A Carus[1], Robert Hamilton[1], Colin S. Harrison[2]

Abstract—**Motorised shoes have been developed to apply chaotic perturbations for gait training. Each shoe comprises four individually controlled actuators, two in the heel and two in the forefoot. Rapid speed of actuator movement has been achieved with the use of a slider-connecting rod-crank mechanism. The mechanism was constructed in a 3D model and checked for component interference using kinematic analysis. Force analysis was undertaken using Euler rotations of each segment in co-ordinate transformation matrices. Component drawings were transferred to a finite element analysis package and factors of safety were applied for a fatigue life of 60,000 steps for each actuator. Latterly that has been extended and one of the pairs of shoes has undertaken 250,000 steps without serious problems. Four pairs of shoes are currently in trials with approximately 100 users. Future work will focus on weight reduction, increased load capacity and extended fatigue life.**

I. Introduction

THE aim of the SMILING project is to develop a training system to improve gait in elderly people by challenging the brain with perturbations [1]-[2] (see section VI for project contract details). The background to this work has been the fruitful outcomes of related research into the improvement of motor learning [3]-[5].

Gait perturbations are applied by motorized shoes which are able to provide independent +/- 4.5 degrees of ankle rotation in both pronation/supination and dorsiflexion/ plantarflexion as well as the possibility of increasing shoe height. The magnitudes of the ankle inclinations and height are coupled to data from chaotic trajectories. Each shoe comprises four actuators (two for the heel and two for the forefoot) to provide stability at heel contact and toe off. The actuators move during the swing phase of gait, which is detected by an integral inertial sensor system. Four pairs of shoes are currently under trial with approximately 100 users.

This paper describes the mechanisms in the shoes and the critical features which have affected their development.

Manuscript submitted 26 June 2010. The research leading to these results has received funding from the European Community's Seventh Framework Programme (FP7/2007-2013) under grant agreement number 215493

[1] Department of Mechanical Engineering, University of Strathclyde, Glasgow, G1 1XJ (corresponding author david.carus@strath.ac.uk +44 141 548 2592; r.hamilton@strath.ac.uk)

[2] Advanced Forming Research Centre, University of Strathclyde, 85 Inchinnan Drive, Inchinnan, Renfrew, PA4 9LJ (c.harrison@strath.ac.uk)

II. Specification

A. Range and Speed of Movement

The specification for the shoes required the actuators to have full movement of 25mm from their fully closed to fully open positions within 250ms, which was the stipulated available time in swing phase for an elderly person. The height gain is calculated for a distance between anterior and posterior actuators of 200mm (for a large man) and 67mm between medial and lateral actuators, so the required height gains are for plantar/dorsiflexion 200 x tan(4.5) = 15.7 mm and for varus/valgus 63 x tan(4.5) = 5 mm, total ~21mm.

B. Load Capacity

The ground reaction forces to which a single actuator could be subjected at heel contact and toe off were calculated for a user body mass of 85kg and the acceleration values given in Table 1. These force values were used in rigid body calculations for the loads in the structure.

TABLE I
GROUND REACTION FORCES

BODY WEIGHT
BW = 85 kg * 9.81 = 834 Newtons
(In British/US units BW = 187 lbs = 13 stones 5lbs)
VERTICAL GROUND REACTION FORCE
Fz = 834 N * 1.2 (estimate of acceleration) = 1,004 Newtons
AP GROUND REACTION SHEAR FORCE
AP share < 25% BW – with a peak of 23% in terminal stance
Fap = 834 * 0.25 = 209 Newtons
ML GROUND REACTION SHEAR FORCE
ML share <10% BW - with a peak of 7% in terminal stance
Fml = 834 * 0.07 * 1.3 (factor of safety) = 76 Newtons
TORSIONAL MOMENT *(pivoting about the vertical axis)*
Too difficult to estimate

C. Application

The users are typically elderly people who prefer to wear soft shoes, such as trainers or suede. The SMILING system meets this preference by allowing a user's own shoe to be firmly strapped to the mechanism by means of a modified crampon. The finished shoes comprise separate anodized heel and forefoot units, firmly bolted to the crampons (Fig.1). Extender bars between the heel and forefoot units allow different shoe sizes to be fitted. Electrical leads for the

motors, the encoders and switches are contained in flexible umbilical cords.

Fig. 1. Completed anodized motorised shoes.
The umbilical cords hold the electrical leads

Brackets attached at the rear of the heel units are included to hold the electronics units, comprising the power supply unit (PSU), motor control unit (MCU) [6], rechargeable batteries, inertial systems (gyroscopes and accelerometers) and the wireless communication system for the waist-supported user control unit (UCU) and/or the operator control unit (OCU).

III. Design

A. Mechanism

Actuator design was based upon the use of a carrier 'A' that is driven by an ACME lead screw 'CD' to drive a slider-connecting rod-crank 'AC-AB-CB' with an offset 'BT' to the crank 'CB'. The offset is used for speed amplification. 'T' is the floor contact point (Fig. 2).

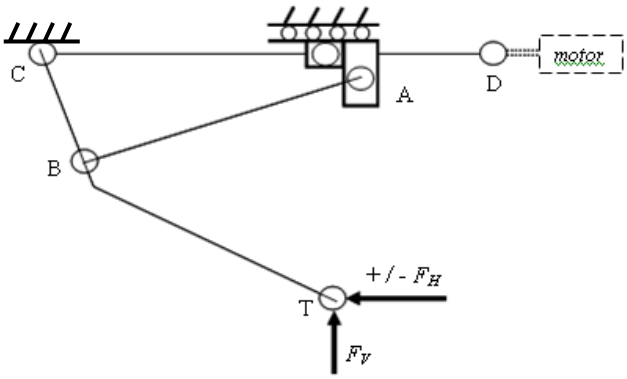

Fig. 2. Actuator mechanism comprising carrier 'A', lead screw 'CD', connecting rod 'AB', crank 'CB' and rigid offset extension to the crank 'BT'

The main advantage of this arrangement is the speed amplification associated with the use of the crank offset. The principal disadvantages are the high bending moments that are generated and in particular the couple generated on the carrier 'A' because the revolute joint at 'A' for the connecting rod cannot be co-incident with the longitudinal bearing that supports the lead screw 'CD' (Figs. 2 and 3).

The actuator must have non-reversible movement, meaning the motor can drive the lead screw but not vice versa. The empirical rule is if the screw pitch is less than 1/3 its diameter, back-driving will not occur. This was checked for the ABSSAC type 2516 lead screw for the major diameter, the root diameter and the mean of the pitch & root diameter. The rule was satisfied and this lead screw was chosen for the application. Table 2 shows that only the ratio for the minor diameter fails the empirical formula and it is unlikely that this is relevant. This provided confidence that the lead screw would exhibit non-reversibility and this was proven in practice.

TABLE 2
LEAD SCREW NON-REVERSIBILITY CALCULATIONS

	Pitch / Diameter
Screw pitch 1.600mm	-
Major diameter 6.350mm	0.25
Root (minor) diameter 4.318mm	0.37
Pitch diameter 5.334mm	0.30
Mean of pitch and root diameter 4.826mm	0.33

The lead screw is driven by a flexible chain drive connected to a dc motor with a 6.3:1 gear ratio and an incremental position encoder. The sprockets for the chain drive provide an additional 1.2:1 speed ratio. The complete arrangement provides the required actuator output speed of 100mm/s. The speed relationship between motor rotation (measured with its incremental encoder) and 1mm increments of the carrier is;

$$\text{lead\_screw\_rotation} := \text{motor\_rotation}\cdot\left(\frac{1}{6.3}\right)\cdot\left(\frac{12}{10}\right)$$

$$\text{carrier\_travel} := \text{lead\_screw\_rotation}\cdot(1.6)$$

$$\text{carrier\_travel} := \text{motor\_rotation}\cdot\left(\frac{1}{6.3}\right)\cdot\left(\frac{12}{10}\right)\cdot(1.6)$$

$$\text{motor\_rotation} := \left[\frac{1}{\left[\left(\frac{1}{6.3}\right)\cdot\left(\frac{12}{10}\right)\cdot(1.6)\right]}\right]\cdot\text{carrier\_travel}$$

For 3.281 motor revolutions, the lead screw rotates 0.625 revolutions and the carrier moves 1mm.

Force analysis was undertaken through the process of transferring coordinates of points in moving segments to an axis system fixed to the shoe structure, using Euler rotations of each segment in co-ordinate transformation matrices. This was done in a MathCAD [7] program 'LINKAGE' written specifically for the project that was used to calculate all bearing forces, the axial force in the lead screw and the magnitude of the couple on the carrier. This couple is particularly high and is ~74 Nm (2 x 2,735 x 13.5mm) which of course has to be opposed by an opposite couple generated on the lips that connect the carrier to its slider

track (Fig. 3). The tensile force in the lead screw is 5,470 Newtons, approximately half the weight of a small car.

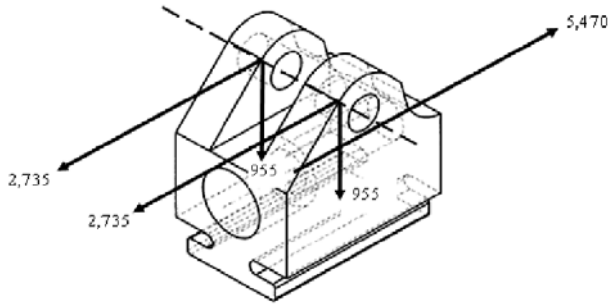

Fig. 3. Forces exerted on the actuator carrier. The two lower lips are supported on a slider track, which has to withstand a couple of 74Nm

A housing machined from a single block of 7000 series aluminium is used to support its two actuators as well as the associated motors, micro-switches, support bracket for the electronics etc. Force analysis revealed that each end of the rear wall of the housing has to support two crank bearing forces of 2,665 Newtons in addition to the 5,470 Newtons reaction force for the lead screw thrust bearing (Figs. 4 & 5).

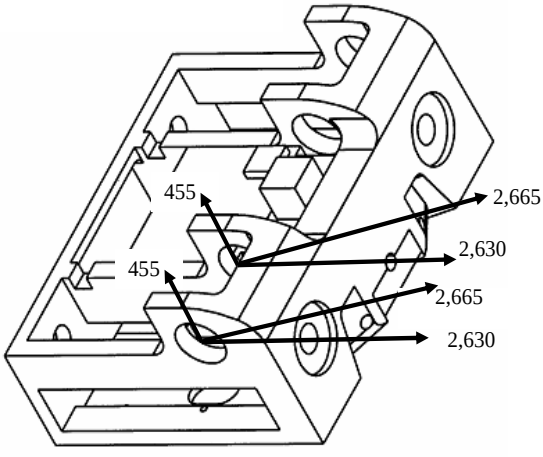

Fig. 4. Bearing forces on lugs that support the crank

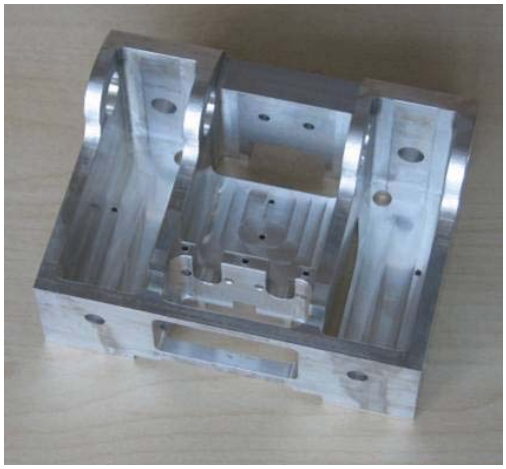

Fig. 5. Single aluminium unit that supports two actuators

B. Stress Analysis

Stress analysis was undertaken using finite element models in the FEA package ABAQUS [8]. The original geometry details produced in Pro/ENGINEER [9] were imported into ABAQUS via the STEP CAD transfer protocol. The finite element model was then generated within ABAQUS. The following series of operations were carried out for each of the components analysed;

(1) Definition of geometry for separate parts
    e.g. base plate and bearing pin
(2) Application of material properties
(3) Assembly of separate parts
(4) Definition of analysis steps
(5) Definition of contact and other interactions between parts
(6) Application of loads and displacement boundary conditions
(7) Solution, memory options and submission of analysis job
(8) Post-processing and visualisation
(9) Results output

A critical part of the analysis reflected the requirement of the trials programme that each shoe should make 60,000 steps, though in fact this requirement was extended to 250,000 steps during the trials. The usual methodology is to use S-N curves, which are plots of number of cycles to failure against allowable stress amplitude of cyclic stress. However the generally available S-N curves are for un-notched polished specimens which are produced from test data and even for these "ideal" S-N curves there is scatter in the experimental data. Hence these ideal curves had to be modified to take into account this variability and to account for other factors also such as surface finish, stress concentrations, operating speeds etc which would exist in the actual component. In effect a factor of safety was applied to the un-notched S-N curve to produce a corrected or notched S-N curve.

Reduced fatigue strength was calculated by applying the formula;

$$\mathbf{S'_N = K_N S_N} \qquad (1)$$

Where S_N is the un-notched or ideal fatigue strength at N cycles, S'_N is the real or reduced fatigue strength for the component at N cycles and K_N is an overall strength reduction factor.

The overall value of K_N is less than one and depends on the factors referred to previously which affect the fatigue strength. Hence

$$\mathbf{K_N = K_a \times K_b \times K_c \ldots \times K_z} \qquad (2)$$

K_N was a factor of safety for fatigue strength. Strength reduction factors for the main support units are given in Table 3. K_r is a strength reliability factor to account for the inherent variability of the experimental data on which the

ideal un-notched S-N curve is based. The ideal curve for K_r=1 equates to a probability of 50% of survival at any number of cycles.

TABLE 3
STRENGTH REDUCTION FACTORS FOR THE MAIN ALUMINIUM SUPPORT UNITS

RELIABILITY R (PERCENT)	STRENGTH RELIABILITY FACTOR KR
Kgr (grain size)	1
Kwe (weld)	1
Kf (stress concentration)	1
Ksr (surface finish)	0.87
K (size effect)	1
Krs (residual stress)	1
Kfr (fretting)	1
Ksp (operating speed)	0.9
Kr (Strength Reliability)	0.81

In the case of the motorised shoes, it was necessary to have a higher probability of survival, R and hence a lower probability of failure so the K_r value had to be reduced. Typical values of K_r and the equivalent probability of survival are given in Table 4.

TABLE 4
STRENGTH RELIABILITY FACTOR AS A FUNCTION OF RELIABILITY LEVEL (FROM COLLINS [10])

RELIABILITY R (PERCENT)	STRENGTH RELIABILITY FACTOR KR
90	0.9
95	0.87
99	0.81
99.5	0.7944
99.9	0.75
99.995	0.69

For the fatigue analysis of the aluminium support units that hold the actuators, the assumption was made that there would be five working pairs of shoes so there would be 20 support units in total (10 heel units and 10 forefoot units). The reliability options were;

(a) For a reliability of 95%, K_r = 0.87; this gives a failure rate of 20 x (1-0.95) = 1 unit failing

(b) For a reliability of 99%, K_r = 0.81; this gives a failure rate of 20 x (1-0.99) = 0.2 units failing (i.e. 1 in 5)

(c) For a reliability of 99.9%, K_r = 0.75; this gives a failure rate of 20 x (1-0.999) = 0.02 units (i.e. 1 in 50)

A reliability value of 99% was chosen, giving the possibility of 0.2 units failing during the trial. Hence Kr = 0.81 was used for the main support units, shown in Table 3.

For the fatigue analysis of the upper crank, connecting rod, carrier & track, again the assumption was made that there would be five working pairs of shoes. Given that there are two of each of these components in each support unit then for five pairs of shoes (with 20 support units) this gives 40 component units. The reliability options were;

(a) For a reliability of 95%, K_r = 0.87; this gives a failure rate of 40 x (1-0.95) = 2 units failing

(b) For a reliability of 99%, K_r = 0.81; this gives a failure rate of 40 x (1-0.99) = 0.4 units failing (i.e. 2 in 5)

(c) For a reliability of 99.5%, K_r = 0.7944; this gives a failure rate of 40 x (1-0.995) = 0.2 units failing (i.e. 1 in 5)

(d) For a reliability of 99.9%, K_r = 0.75; this gives a failure rate of 40 x (1-0.999) = 0.04 units failing (i.e. 1 in 50)

It was decided that the failure rate of the upper crank, connecting rod, carrier and track should be the same as the main support units hence the value of Kr was chosen to be 0.7944 for these components, shown in Table 5.

TABLE 5
STRENGTH REDUCTION FACTORS FOR THE UPPER CRANK, CONNECTING ROD, CARRIER AND TRACK

RELIABILITY R (PERCENT)	STRENGTH RELIABILITY FACTOR KR
Kgr (grain size)	1
Kwe (weld)	1
Kf (stress concentration)	1
Ksr (surface finish)	0.87
K (size effect)	1
Krs (residual stress)	1
Kfr (fretting)	1
Ksp (operating speed)	0.9
Kr (Strength Reliability)	0.7944

FEA was carried out for each component. The material used throughout was 7075 – T651 aluminium alloy and its properties are;

Young's Modulus (N/mm^2)	70e3
Poisson's Ratio	0.3
Ultimate Strength (N/mm^2)	572
Yield Stress (N/mm^2)	503

The ideal or un-notched fatigue curves for this material were obtained using a standard procedure based on the ultimate strength of the material described in Norton [11]. These ideal curves where then modified using equation (1) to obtain a corrected or notched S-N curve. The allowable stress amplitude obtained from the S-N curve was found to be 256 N/mm^2 (K_N = 0.634). The methodology used was very similar to the procedure used in the European Pressure Vessel Code [12,13] and SAE Design Handbook [14] which use the von Mises stress for assessment procedures. The ASME Pressure Vessel Code [15] also uses a similar procedure but is based upon the stress intensity (or Tresca).

For each finite element model, critical areas of high stress were identified and a fatigue assessment carried out to determine the predicted fatigue life. Specifically the points of highest von Mises stress, principal tensile and principal compressive stress where identified in the model. In all cases the point of maximum von Mises stress, S_{vm} coincided with either the maximum principal tensile or maximum compressive stress. An appropriate von Mises stress amplitude was then calculated based on the von Mises stress at each point using equation (3).

$$\sigma_a = \frac{S_{vm}}{2} \qquad (3)$$

It can be seen in equation (3) that the stress amplitude was half the peak von Mises stress, S_{vm} since it is assumed that the load starts from zero, rises to a peak, and then falls back to zero. A modified von Mises stress amplitude was then calculated to take into account the mean stress effect of the load cycle using equations (4) and (5).

$$\sigma_{eqv} = \sigma_a \frac{Su}{Su - \sigma_m} \qquad (4)$$

$$\sigma_m = \frac{S_1 + S_2 + S_3}{2} \qquad (5)$$

S_U is the ultimate stress of the material, σ_m is the mean stress which is half the sum of the principal stresses, S_1 is the first principal stress, S_2 is the second principal stress and S_3 is the third principal stress.

Equation (3) is used because the mean stress is tensile and using the Goodman diagram [16], it was assumed that the compressive mean stress would not affect fatigue strength whereas a tensile mean stress would cause a decrease in fatigue strength. This modified von Mises stress amplitude was used, with the appropriate notched S-N curve to calculate the predicted cycles to failure. Where the peak von Mises stress, S_{vm} was greater than the yield stress then the modified von Mises stress amplitude was assumed to be the yield stress, which implies a very low fatigue design life.

The couple on the lead screw carrier that has to be resisted by the slider support gives rise to the maximum value of von Mises stress on the lower radius of the carrier. The magnitude of the contact stress values are above yield, leading to localised surface pitting (Fig. 5).

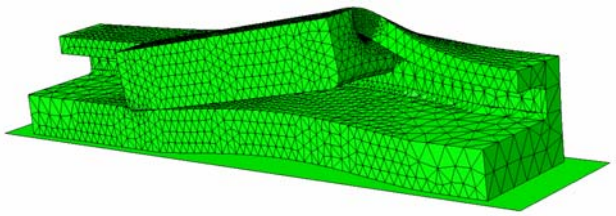

Fig. 5. Deformed shape for the carrier and its support slide. Localised Herzian contract stresses are generated

The resistive couple is provided by hardened steel bolts screwed through the crampons into captive nuts. Hence the crampons are integral parts of the structures. These class 10.9 bolts have a proof stress of 830 MPa and a UTS of 1,040 MPa, which is double that for 7075 aluminium (UTS = 580 MPa).

One pair of shoes that had been used for 250,000 steps without failure was examined and it was found that the localized Herzian contact stresses had not resulted in significant damage. In fact, the damage that was present was wear caused primarily through lack of lubrication (Fig. 6)

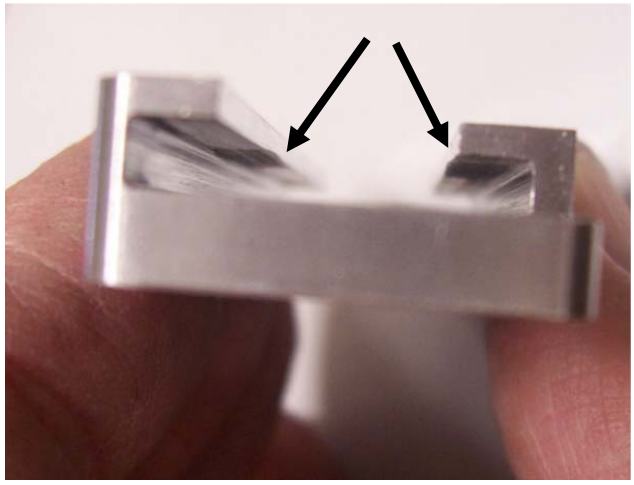

Fig. 6. Damage visible on the inside surface of the carrier's support slide caused by a combination of localized contact stress and wear

C. Floor Contact Rocker

The rigid body force analysis and FEA were conducted using a relatively simple crank offset arrangement but considerable improvement was later identified and achieved during the manufacturing process by introducing a rocker (Fig. 7). With this feature, the floor contact pressure point is situated near the axis of the crank, thereby reducing forces throughout the structure. This means that the force magnitudes that were used in the FEA analysis were in fact too large and need to be re-calculated in future work.

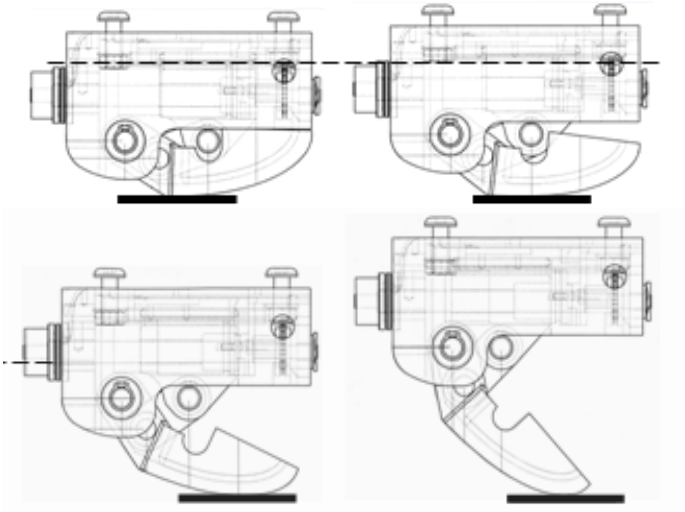

Fig. 7. Rocker used in the mechanism for floor contact

It is noteworthy that users have reported they feel comfortable with the rocker at the time of forefoot roll-over. There is a natural feel in the transition from stance to swing.

IV. APPLICATION OF TAGUCHI METHOD FOR DESIGN, MANUFACTURE AND ASSEMBLY

The Taguchi method for design and manufacture was followed using the guideline “the quality of a product is improved by minimizing the effect of the causes of variation without eliminating the causes” [17]. Inevitably, there are variations in component tolerances and alignments that cannot be eliminated in manufacture so instead their effect has been minimized through the introduction of features that can accommodate variations. Two methods have been used; first, the flexible low-stiffness chain in the drive between the motor and the lead screw has the dual effect that its length can be adjusted to alter free-play in movement and also reduce mechanical impedance; second, the actuator’s fully open and fully closed positions that have to be detected by the micro-switches can be adjusted by bending the contact levers attached to the switches. The structure is modular and parts can be removed and replaced with simple hand tools.

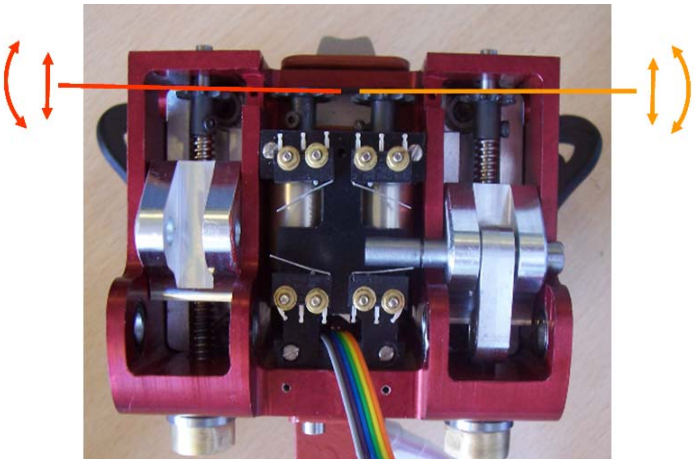

Fig. 8. Taguchi method applied to the shoe structure. Variations in component sizes and misalignments are compensated by altering chain tension, chain alignment and microswitch lever positions

V. FUTURE WORK

At the time of submitting this paper, the motorized shoes were performing well in user trials, with few problems. Nevertheless, it is recognized that the shoes are too heavy. The mass of a complete shoe (the mechanism, battery and electronics) is 1.9kg and weight reduction will be the primary focus of future work. Other work will concentrate on raising the allowed mass of a user. This is currently set at 85kg to prolong fatigue life.

VI. SMILING PROJECT

The project “Self Mobility Improvement in the eLderly by counteractING falls” (SMILING) is part of the European Commission's 7th RTD Framework Programme – Specific Programme Cooperation, Theme 3 "Information and Communication Technologies", Objective ICT2007.7.1 "ICT and Ageing", contract number 215493.

ACKNOWLEDGMENTS

The authors are delighted to acknowledge the support of the project co-ordinator Dr Fiorella Marcellini, INRCA (Italian National Institute of Aging) and their fellow partners INRCA (www.inrca.it), Ab.Acus (www.ab-acus.com), Centre Hospitalier Universitarie Vaudois CHUV (www.chuv.ch), Stichting Imec-Nl (www.holstcentre.com), École Polytechnique Fédérale de Lausanne EPFL (www.epfl.ch), Faculty of Health Sciences at Ben-Gurion University of the Negev MISHAN (www.mishan.co.il), Step of Mind SOM (www.stepofmind.com), Geriatric Center Kosice GCKOSICE (www.gckosice.sk), Technical University of Kosice TUKE (www.tuke.sk) and Alma Mater Studiorum, Università di Bologna UNIBO (www.unibo.it)

REFERENCES

[1] Bulgheroni M, d'Amico E, “The SMILING system: a comprehensive approach to the perturbation of walking", submitted ICABB2010

[2] Bulgheroni M, D'Amico E, Bar-Haim S, Carus D, Harrison C, Marcellini F, “The SMILING project: Prevention of falls by a mechatronic training device”, Telehealth and Assistive Technology, November 2-4 2009, Cambridge, Massachussets, USA

[3] Bar-Haim S, Harries N, Belokopytov M, Lahat E, Kaplanski J, “Random perturbation: A potential aid in treatment of children with cerebral palsy,” *Disability & Rehabilitation*, vol. 30, issue 19, pp. 1420 – 1428, 2008

[4] Emken J L, Reinkensmeyer D J, “Robot-Enhanced Motor Learning: Accelerating Internal Model Formation During Locomotion by Transient Dynamic Amplification,” *IEEE Trans. Neural Syst. Rehab. Eng*., vol. 13, no. 1, pp. 33-39, March 2005

[5] Scheidt R A, Dingwell J B, Mussa-Ivaldi F A, “Learning to Move Amid Uncertainty,” *J Neurophysiol*., vol. 86, no. 2, pp. 971-985, August 2001

[6] Simsik D, Drutarovsky M, Galajdova A, Galajda P, Embedded Microcontroller Unit for Gait Rehabilitation Shoes, submitted ICABB2010

[7] MathCAD manual, version 13, PTC HQ, Needham, MA 02494, USA

[8] ABAQUS Analysis Manual, version 6.8, Dassault Systemes Simulia Corp., Providence, RI, USA, 2008.

[9] Pro Engineer, version 2.4, 2006

[10] Collins J A, Mechanical Design of Machine Elements and Machines, John Wiley & Sons, pp. 49, 2003.

[11] Norton RL, Machine Design: An integrated approach, 2nd Edition, Prentice Hall, pp. 355-356, 2000.

[12] En 13445 : Part 3 – European pressure vessel code : Unfired pressure vessels, 2006.

[13] Zeman JL Pressure Vessel Design: The Direct Route, Elsevier Science, Chapter 7, pp. 101-143, 2006.

[14] SAE Fatigue Design Handbook, 3rd Edition, Society of Automobile Engineers, PA, USA, 1997.

[15] ASME, Boiler and Pressure Vessel code section VIII, American Society of Mechanical Engineers, New York, USA, 2006.

[16] Collins J A, Mechanical Design of Machine Elements and Machines, John Wiley & Sons, pp. 59-63, 2003.

[17] Feng Q, Kapur K C, *Quality Engineering: Control, Design and Optimisation*. ch. 13, pp 171-186, in *Handbook of Performability Engineering* Krishna B. Misra (editor) ISBN 978-1-84800-130-5, Springer-Verlag, 2008